E-ISSN : 2541-5794
P-ISSN : 2503-216X

Journal of Geoscience,
Engineering, Environment, and Technology
Vol 9 No 2 2024

RESEARCH ARTICLE

Magma Petrogenesis Study Based on Morphology and Texture Of Zircon Minerals: Case Study At The Causative Intrusive In The HLE Porphyry Copper-Gold Prospect, Sumbawa Island, Indonesia

Fadlin[1,*], Raden Isnu Hajar Sulistyawan[2], Arifudin Idrus[2], Raden Muhammad Asfaro[1], Hernani Vitorino Nhatinombe[4], Wildan Nur Hamzah[5]

[1] *Department of Geological Engineering, Jenderal Soedirman University, Purwokerto, Indonesia*
[2] *Geological Museum, Geological Agency, The Ministry of Energy and Mineral Resources Republic, Indonesia*
[3] *Department of Geological Engineering, Universitas Gadjah Mada, Yogyakarta, Indonesia*
[4] *Department of Geology, Eduardo Mondlane Universite, Maputo, Mozambique*
[5] *Akita University, Akita City, Japan*

* Corresponding author : fadlin@unsoed.ac.id
Tel.: +62-281-6596801, 6596700; Fax.: +62-281-6596801, 6596700
Received: Jun 16, 2023; Accepted: May 22, 2024.
DOI: 10.25299/jgeet.2024.9.2.13248

Abstract

The zircon mineral is one of the accessory minerals within igneous rocks for its ability to resist hydrothermal and metamorphic processes. By examining their morphology and texture, zircon minerals can provide valuable insights into magma's petrogenesis, including temperature and composition. Two methods used to reach the research objectives include Petrography and SEM-CL analysis of the zircon grain from the diorite porphyry of the HLE prospect. On the basis of Petrography observation, the grain size of zircon ranges from 50 to 300 µm in size, and most have a transparent to grey color with prismatic, non-prismatic euhedral-subhedral elliptical, and non-prismatic rounded in shape. The zircon crystal typologies from the diorite porphyry are classified into S10, P2, S12, S13, S16, and S17 types, indicating the wide range of the crystallization temperature of zircon, ranging from 700 to 800 °C. The zircon from the diorite porphyry of the HLE prospect shows the medium values of pyramids typology, which is {101} = {211}. It corresponds to a medium Al/Na + K ratio (A index) value, indicating zircon as a product from the calc-alkaline magmas series. The trend of the calc-alkaline/sub-alkaline in typology suggests crustal sources mixed with mantle material. Furthermore, based on SEM-CL analysis the zircon shows dominantly oscillatory zoning with thin bands, and some grains show weak zoning in the outer core, typical of magmatic zircon. Moreover, the presence of lamellae texture of magnetite-ilmenite mineral under the scanning electron microscopy (BSE image) can be interpreted as the magma related to the high oxidizing magma.

Keywords: Zircon morphology, Pupin methods, petrography, cathodoluminescence (CL), Sumbawa Island

1. Introduction

Zircon is one of the accessory minerals within igneous rocks, zircon is known for its resistance to hydrothermal and metamorphic processes (Rubatto, 2017; Li et al., 2023). Based on previous studies related to granitic rock by Pupin, 1976; Pupin and Turco, 1972; Pupin and Turco 1975. Generally, the crystallization temperature and aluminum-alkali balance in the formation of zircon can influence the variance of the crystal morphology. This has led to using zircon populations as tracers of the petrogenesis of granitic magmas. Various morphological parameters can be used to identify petrogenetic information, such as crystal habits, which are variable among them. Pupin and Turco, 1972; Pupin and Turco, 1975; Pupin, 1976; and Pupin, 1980, 1985; and Pupin, 1988 have all pointed out this important petrogenetic information. Several geoscientists have conducted similar studies related to that topic, such as Dias et al., 2002, Martins et al., 2009; 2013; 2014 using the classic method by Pupin (1980) against the information of petrogenetic related to geochemistry and stable isotopic data. Our research purpose is to apply morphological study of zircon in order to understand the petrogenetic of the diorite rock as a causative intrusion at the HLE prospect relating to temperature formation and magma petrogenetic.

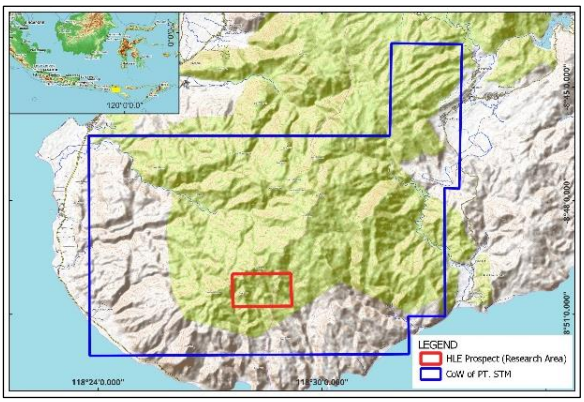

Fig. 1. Sumbawa Timur Mining tenement area of Hu'u district, where the HLE prospect is situated.

The research area is in Hu'u district, Dompu Regency, Sumbawa Island, Indonesia, within the tenement area of

Sumbawa Timur Mining Company (PT. STM). The research area is approximately 30 km south of the Dompu regency and 75 km southwest of Bima city (Fig. 1). It takes approximately 45 minutes to fly from Mataram to Bima city and two hours by car to reach Hu'u.

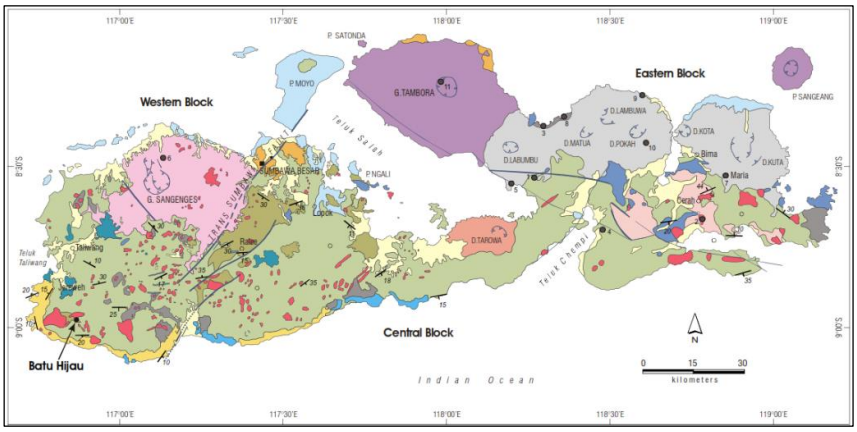

Fig. 2. Illustrates a simplified geological map of Sumbawa Island, modifications from Suratno (1994, 1995), Sudradjat (1998), and Garwin (2000).

1.1 Geological Background

The Indonesian Geological Survey has published Sumbawa Island's simplified geological map and stratigraphical column (Suratno, 1994; Sudradjat et al., 1998) (Fig. 2). The island of Sumbawa spans an expanse of more than 15.000 square kilometers, characterized by an east-west axis stretching roughly 270 kilometers. Numerous volcanoes, including the tallest, Mt. Tambora (2851 MASL), punctuate its surface. According to Garwin (2000), the morphology and geology of Sumbawa Island are categorized into three blocks, including western, central, and eastern blocks. These blocks are demarcated by the northwest arc transverse and Trans Sumbawa fault system, which is situated adjacent to the margin of the Sunda continental shelf (Barberi et al., 1987). In the western block, near Batu Hijau, the crustal thickness ranges from 14-16 km, while in the central block, specifically in the Humpa Leu East (Hu'u district and surrounding area), it extends from 20-23 km. The increased thickness of the central block aligns with its subsidence relative to the western and eastern blocks.

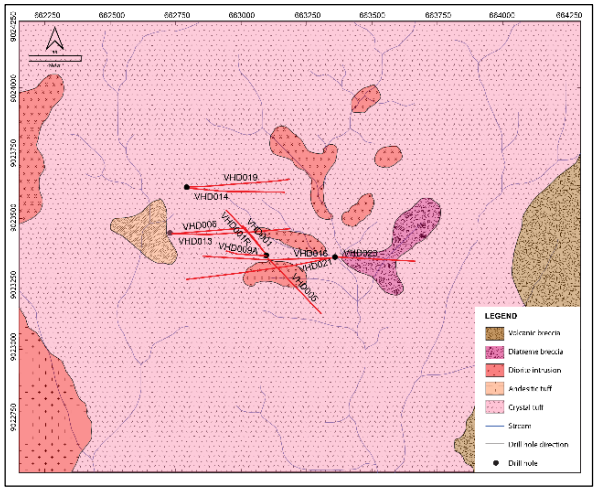

Fig. 3. Geological map of the research area (modified from PT. Sumbawa Timur Mining, 2018).

The thickness of the western block is going increase western to the north, while the eastern block going increase to the south (Barberi et al., 1987). The interpretation implies that the southern portion of the western block has been uplifted and tilted northward, mirroring the uplift and southward tilting observed in the northern segment of the eastern block. In contrast, the central block, having subsided, and the southerly tilted eastern bloc exhibit elevated levels of crustal exposure. This interpretation is substantiated by the distribution patterns of rock types and the observed modes of hydrothermal alteration in Sumbawa (Garwin, 2000). The Sumbawa Island region exhibits two prominent calc-alkaline volcanic sequences dating from the Neogene to Early Pleistocene era, as depicted in Figure 2. These sequences are primarily composed of an Early to Middle Miocene volcanic and volcano-sedimentary succession, featuring a substantial volcaniclastic component (Garwin, 2000).

The sequences of the volcanic product are developed by andesitic, dacitic, and rhyolitic composition which are shown at Lopok, Jereweh, and Cerah Area (Suratno, 1994).

The andesitic volcanic are characterized by lower greenschist facies metamorphism which is composed of key metamorphic minerals including mica, calcite, and epidote. The andesitic volcanic sequence in the eastern part of Sumbawa Island is superimposed by dacitic pyroclastic and sedimentary-volcanic rock (Suratno, 1994). These sequences typically exhibit dips of less than 20°, but in some localities, the dip can reach up to 45°, with thicknesses exceeding 500 meters (Garwin, 2000). The northern section of the island is host to Quaternary volcanoes, with their alkalinity exhibiting an increasing trend over time. The Pleistocene volcanoes in the northern-northeastern part of Sumbawa display calc-alkaline compositions, while Sangenges and the historically active Tambora and Sangeang Api volcanp exhibit shoshonitic affinities (Foden and Varne, 1980; Barberi et al., 1987). Numerous type of intrusions with a compositional range from mafic to felsic have been identified within Sumbawa Island. The presence of the intrusion rock at the eastern block and eastern of the central block is less than the western block and the western part of the central block. The intrusions rock are characterized by calc-alkaline magma series with diorite, basaltic andesite, quartz diorite, tonalite, granodiorite, and hypabyssal dacite as a product. Furthermore, the dacitic and andesitic volcanic sequence of Eastern

Sumbawa has been intruded by that intrusion. On the basis of cross-cutting relationships and radiometric dating and cross-cutting relationship shows that these intrusion ages range from Middle Miocene to Pliocene (Garwin, 2000). According to K/Ar radiometric dating, the quaternary volcanic lava from Sangenges and Tambora volcano ages range from 1.71±0.05 to 0.043 ± 0.02 ma (Barberi et al., 1987). Whole rocks and minerals of active Sangeang Api excess ^{226}Ra. Suggest by ^{226}Ra – ^{230}Th-Ba data, the magmatic evolution beneath the arc volcano occurs over timescales of about 2000 years (Turner et al., 2003).

The geological framework of the Hu'u district, characterized by a paleo-volcanic morphology originating from Puma and Wawosigi volcano products. According to Sundhoro et al, (2005). Fusion track dating of Puma lava samples indicates an age of 5.8 ± 0.2 million years. The Hu'u district is surrounded by lowlands and coastal plains, and the highest elevation of the mountains in this district reaches approximately 1020 MASL. The geological composition of the Hu'u district comprises andesite lava and breccias with interspersed sandy tuff, tuff, and tuffaceous sandstone (Ratman & Yasin, 1978; Sudrajat et al. 1998). Geological mapping (PT. STM, 2018) and Landsat imagery studies have classified the Hu'u district into eleven lithological units. During the Early Miocene, the activity of calc-alkaline magmatism decreased, caused by extensive erosion and sedimentation formation. The mineralization at the Sunda-Banda belt is generally linked to the magmatism of the tectonic island arc boundary (Carlile and Mitchell, 1994; Setijadji et al., 2006; Setijadji and Maryono, 2012; Maryono et al., 2018). The transition zone between Sunda and Banda Arc is still unknown, but some scientists suggested that the location is between Flores and Sumbawa Island. The tectonic setting, particularly in the eastern part of the Sunda arc, is still debatable, whether it is related to an island arc or an active continental arc. Hamilton, 1979; Katili, 1975 proposed that arcs relate to the continental arc. This perspective is supported by several publications, including Reubi et al. (2002), Gertisser & Keller (2003), Elburg et al. (2004), Gardner et al. (2013), and Fadlin et al. (2018; 2021; 2023).

Lithologically, the HLE porphyry Cu-Au prospect is composed of by sequences of volcanic rocks, including tuffs (andesitic & crystalline), volcanic breccia, subvolcanic intrusions, diorite intrusions, and andesitic lava (PT. STM 2018). The existance of diorite intrusion as a window suggests that the erosion in this area is not too deep and occurs within a subvolcanic environment (refer to Fig. 3).

Diatreme breccia in research area covering about 500m with orientation southwest-northeast spreading, which is formed by post intrusion process, evidenced by including intrusive rock fragments within the breccia.

Typically, the mineralization in the research area is related to porphyry Cu deposit, with characterized by hypogene mineralization and multiphase diorite porphyry intrusion which can be divided into three phases including early, intemeriate, and late mineral phases (Sillitoe, 2012). The early porphyries exhibit an average composition of 0.5 percent Cu and 0.5 grams per ton Au. In contrast, the inter-mineral porphyries have a significantly lower grade, Cu averaging from 0.2 to 0.3 percent and 0.2 to 0.5 grams per ton Au. However, the eastern side of the intrusion shows a much higher gold content, averaging 0.3 percent Cu and 1 gram per ton Au. The late mineral stages are nearly barren, containing only 0.1 percent Cu and 0.01-0.05 grams per ton of gold (Sillitoe, 2012). As part of a previous project (Fadlin et al., 2023), the author also has identified the mineral constituents of diorite intrusive rocks in the research area. Through petrographic observations, the study revealed a multiphase intrusion characterized by two distinct types of intrusive rock: quartz diorite and diorite porphyry (Fadlin et al., 2023).

2. Sampling and Analytical Method

Samples for this research were collected from intrusions, representing multiple intrusion phases (early, intermediate, and late) at the HLE prospect. Approximately 2 kg of diorite porphyry from three borehole samples (VHD006/500-502, VHD009A/250-252, and VHD001R/600-602) underwent crushing and milling processes to achieve a particle size of < 300 µm. Conventional techniques, such as crushing, panning, magnetic separation, and heavy liquid (utilizing sodium poly-tungstate), were employed to separate zircon grains from the particle, followed by a meticulous handpicking technique using a microscope. Zircon that has been separated, placed in epoxy resins, and polished to reveal its inside. We used polished sections of samples to facilitate mounting into SEM specimen holders approximately 1 cm thick. The polish section samples were also polished with 3 m and 1 m diamond polish. Two observation methods that are used to reach the research objectives include Petrography observation and SEM-CL analysis. Petrography observation is purpose to determine the morphology and typology of zircon mineral using a Nikon ECLIPSE LV100N POL, and the SEM-CL method was also used to understand the zircon mineral's internal texture. In addition, the sample was coated by the carbon coating method before going to analysis under the SEM-CL method. The Oxford Instrument JEOL JSM-6610 SEM-EDS equipment was used for this analysis. These assessments were conducted at the Economic Geology Laboratory, Department of Earth Resource Science, International Resource Sciences Graduate School, Akita University, Japan.

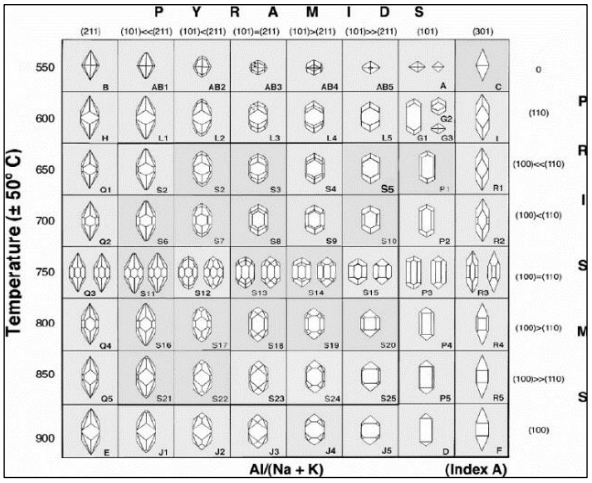

Fig. 4. Zircon typological classification proposed by Pupin (1980)

The zircon typology will be classified using the Pupin classification method to understand magma petrogenesis (Fig. 4). Zircon typological classification proposed by Pupin (1980) show the relationship an index A reflects the

Al/alkali ratio, controlling the development of zircon pyramids, whereas temperature affects the development of different zircon prisms. The methodology employed in this study was initially developed for magmatic zircon associated with granitic rock. However, in the current investigation, this method is adapted to analyze magmatic zircon derived from diorite porphyry. This modification allows for applying the established technique to the specific geological context of the diorite porphyry samples under examination.

3. Result and Discussion

3.1 Morphology of Zircon

Under transmitted light microscope images, the zircon grain of porphyry intrusion from the HLE prospect shows variation in the external morphology. The zircon is grey to transparent in color, the size ranges from 50 to 300 µm. The morphology of zircon grain varies within a single rock sample from a prismatic, non-prismatic euhedral-subhedral elliptical, and non-prismatic rounded. The zircon crystal typologies are classified based on "Pupin diagram", from the relative development of prismatic form ({100} vs. {110}) and the pyramidal form ({211} vs. {101}), which shows that the HLE zircon crystals are classified as S10, P2, S12, S13, S16, and S17 (Fig. 5). A zircon typological classification corresponds to a geothermometric scale based on the crystal faces (Pupin, 1980). The ratio of Al/Na + K (A index) contributes to the development of pyramidal faces.

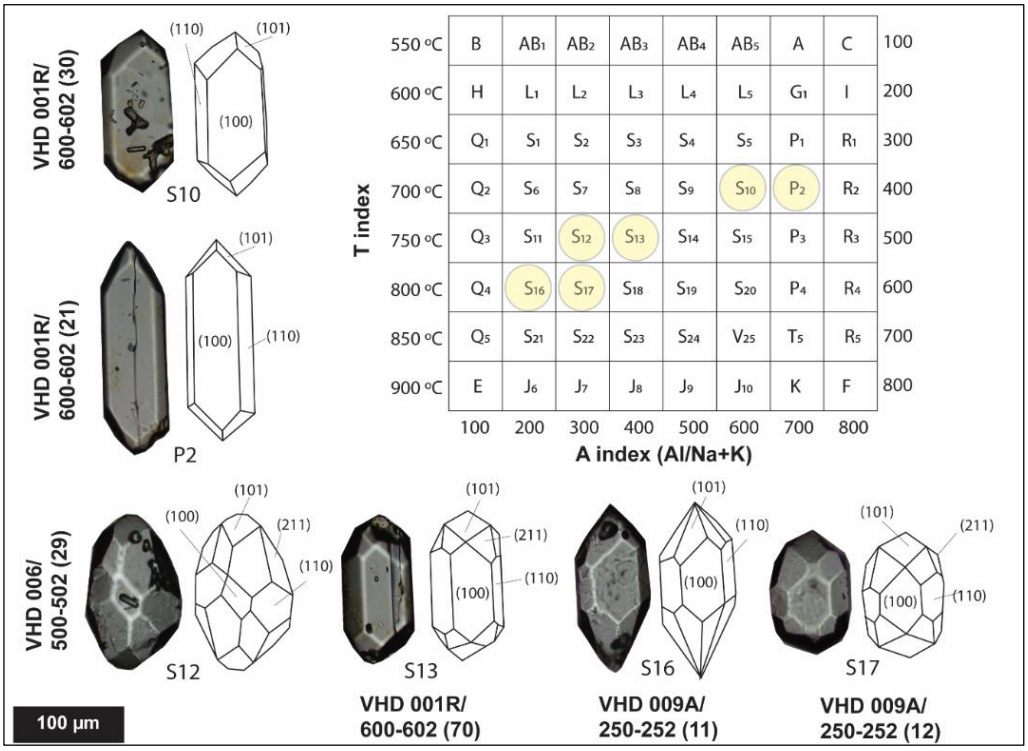

Fig. 5. A proposed typological classification of zircons from diorite porphyry of HLE prospect (after Pupin, 1980). Index A represents the Al/(NA+K) ratio (100-800) which is responsible for the development of zircon pyramids, while the form of the prism is influenced by temperature. The HLE zircon typology includes S10, P2, S12, S13, S16, and S17 (yellow box).

The T index represents the zircon crystallization temperature, which is a control for the prismatic faces. A high T index ({100} prism) implies a higher temperature than a low T index ({110} prism). (Martins et al., 2014; Pupin, 1980). The external structure of the HLE zircon shows slightly more variation on prism typology values, which are from ({100} < {110}) to ({100}> {110}), indicating the wide range of the crystallization temperature of zircon, ranging from 700 OC to 800 OC (Pupin, 1980).

The zircon typology study can interpret the magma affinity series, which refers to the ratio of Al/Na + K (A index). The high Al/Na + K index is related to the alkaline magma series, and the medium index of Al/Na + K is related to the calc-alkaline magma series. . Similarly, the causative intrusion geochemistry of various porphyry Cu-Au prospects or deposits throughout the eastern Sunda arc, such as Kumbokarno (Aldan et al., 2022), Tumpangpitu (Harrison et al., 2018), Batu Hijau (Idrus et al., 2007; 2009), and Brambang (Idrus et al., 2021), demonstrates this. In contrast, a low Al/Na + K index is related to the tholeiitic magma series (Pupin, 1980). Zircon typology from Pupin, 1980 shows an effective and efficient for applying magma genesis study, especially in the case of magma affinity and the formation of zircon temperature. The HLE zircon shows the medium values of pyramids typology, which is {101} = {211} (Fig. 5). It corresponds to a medium value of the Al/Na + K ratio (A index), indicating zircon as a product from the calc-alkaline magmas series (Martins et al., 2014). Furthermore, the trend of the calc-alkaline or sub-alkaline in typology suggests crustal sources mixed with mantle material (Fig. 6)

It is in agreement with previous research, which analyzed magma affinity using whole rock geochemistry to show that the rock affinity in the research area is classified as calc-alkaline series, with some evidence of magma contamination by the mantle (Carlile and Mitchell, 1994; Maryono et al., 2018; Setijadji et al., 2006; Setijadji and Maryono, 2012; Fadlin et al., 2013).

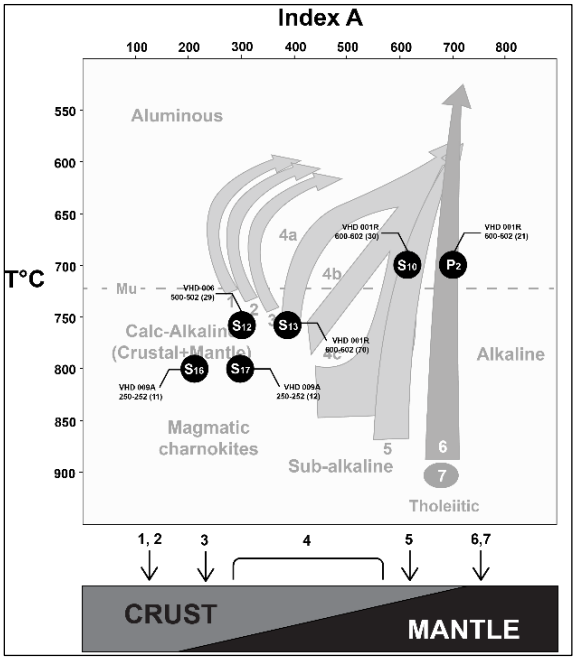

Fig. 6. Typology zircon populations from diorite porphyry of HLE prospect diagram (Modified Pupin, 1988). Crustal origin (orogenic): (1) aluminous rock; (2) (sub) autochthonous rock; (3) intrusive aluminous rock. Calc-alkaline rock (crustal + mantle origin) (subduction-related): (5) sub-alkaline series granites. Mantle origin (within plate): (6) alkaline series and (7) tholeiitic series

3.2 Internal Texture of Zircon

Several zircon grains have mineral and melt inclusions, and a few grains have bubble inclusions (Fig. 7). Based on SEM-EDS analysis, the mineral inclusions consist of apatite, magnetite-ilmenite mineral with lamellae texture, the size varying from 5 µm to 30 µm. Melt inclusions occur in every grain of zircon, with 30-100 µm in size (Fig. 7B). Potassium feldspar, quartz, glass, and Fe-oxide are also present and occur together with the melt inclusions, 3 to 15 µm in size (Fig. 7B).

Several zircon grains have mineral and melt inclusions, and a few grains have bubble inclusions (Fig. 7).

Based on SEM-EDS analysis, the mineral inclusions consist of apatite, magnetite-ilmenite mineral with lamellae texture, the size varying from 5 µm to 30 µm. Melt inclusions occur in every grain of zircon, with 30-100 µm in size (Fig. 7B). Potassium feldspar, quartz, glass, and Fe-oxide are also present and occur together with the melt inclusions, 3 to 15 µm in size (Fig. 7B). The present of lamellae texture of magnetite-ilmenite mineral can be interpreted that the magma related to the high oxidizing magma. Magmas with a high oxidation condition are important for porphyry Cu-Au formation and are usually found in either arc or collisional settings (Cooke, 2005; Sillitoe, 2010; Sun et al., 2015). A high oxidation magma constitutes the one critical component in the production of porphyry Cu-Au deposits, aside from water saturation. (Richards, 2011; 2015; Richards et al., 2012; Chiaradia & Caricchi, 2017; Nevolko et al., 2021). Magma with high oxidation conditions tends to extract more Ce from the source rocks during melting (Sun et al., 2015; Hattori, 2018).

The cathodoluminescence (CL) imaging is used to describe the internal structure of zircon grains. Primary magmatic oscillatory zoning (growth zoning) is the most common type of zoning that shows a dark and bright banding texture (Fig. 7A). Under images of SEM-CL and Backscattered Scanning Electron Microscope (BSE), the HLE zircon shows dominantly oscillatory zoning with thin bands, and some grains show weak zoning in the outer core, typical of magmatic zircon (Martins et al., 2014). A few grains show continuous thin bands zoning from the core to the rim (Fig. 7A). A thin band zoning is common and occurs around a larger core, and some zircons also show weak magmatic zoning in the core, followed by thin bands zoning in the outer rim (Fig. 7A). Furthermore, several grains show a sector zoning in images (Fig. 7A) which show a different brightness on different facets. There are several causes of crystal sector zoning, including differences in the crystal growth rate ratio to element diffusion near the surface of the crystal, differences in adsorption of the cation on face surface, and crystallization force (Watson, 1996; Levashova et al., 2021).

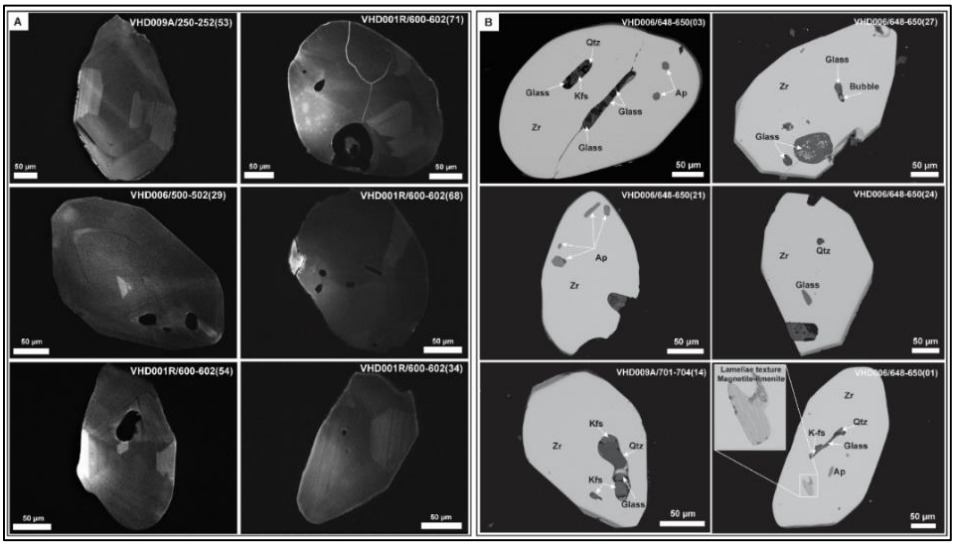

Fig. 7. Representative CL-Images (A) and BSE images by SEM analysis of zircon from diorite porphyry of HLE prospect which showing an inclusion of a several minerals such as apatite, quartz, glass (melt) and lamellae texture of magnetite-ilmenite (B). Abbreviation: Zr= Zircon, Ap= Apatite, Qtz= Quartz, K-fs= Potassium feldspar

4. Conclusion

- The zircon crystal typologies from the diorite porphyry are classified into S10, P2, S12, S13, S16, and S17 types, indicate the wide range of the crystallization temperature of zircon, ranging from 700 to 800 °C.
- The zircon from the diorite porphyry of the HLE prospect shows the medium values of pyramids typology, which is {101} = {211}. It corresponds to a medium Al/Na + K ratio (A index) value, indicating zircon as a product from the calc-alkaline magmas series.
- The trend of the calc-alkaline series magma in typology suggests that the material from crustal which slightly contamined by the mantle source. Furthermore, based on SEM-CL analysis the zircon shows dominantly oscillatory zoning with thin bands, and some grains show weak zoning in the outer core, typical of magmatic zircon.
- Moreover, the present of lamellae texture of magnetite-ilmenite mineral under the scanning electron microscopy (BSE) can be interpreted that the magma related to the high oxidizing magma.

Acknowledgements

The research team expresses gratitude to Sumbawa Timur Mining and VALE management for their collaboration and for generously granting permission to conduct this study within their tenement area.

References

Aldan, A.F., Idrus, A., Takahashi, R., Kaneko, G., 2022. High-Sulfidation Epithermal – Porphyry Transition in the Kumbokarno Prospect, Trenggalek District , East Java, Indonesia: Constraints from Mineralogy, Fluid Inclusion, and Sulfur Isotope Studies. Resource Geology 72: 1-25. https://doi.org/10.1111/rge.12289

Barberi, S., Bigioggero, B., Boriani, A., Cattaneo, M.R., Cavallin, A., Eva, C., Cioni, R., Gelmini, R., Giorgetti, F., Iaccarino, S., Innocenti, F., Marinelli, G., Slejko, D., & Sudradjat, A.,1987. The Island of Sumbawa; a major structural discontinuity in the Indonesian Arc. *Bollettino Della Societa Geologica Italiana, 106*, 547-620.

Benisek, A. and Finger, F.,1993. Factors controlling the development of prism faces in granite zircons- a microprobe study Contrib. Mineral. Petrol., 114 (2), pp. 441-451

Carlile, J.C., and Mitchell, A.H.G.,1994. Magmatic arcs and associated gold and copper mineralization in Indonesia. Journal of Geochemical Exploration, 50, 91-142. https://doi.org/10.1016/0375-6742(94)90022-1

Chiaradia, M., and Caricchi, L., 2017. Stochastic modelling of deep magmatic controls on porphyry copper deposit endowment. Sci. Rep. 7:44523. https://doi.org/10.1038/srep44523

Cooke, D.R., Hollings, P. and Walshe, J.L., 2005. Giant deposits characteristics, distribution, and tectonic controls: Economic Geology, 100, 801-818.

Dilles, J.H., A.J.R. Kent, J.L. Wooden, R.M. Tosdal, A. Koleszar, R.G. Lee, and L.P. Farmer., 2015. Zircon compositional evidence for sulfur-degassing from ore-forming arc magmas. Economic Geology, 110, p.241–251. https://doi.org/10.2113/econgeo.110.1.241

Elburg, M.A., van Bergen, M.J., Foden, J.D., 2004. Subducted upper and lower continental crust contributes to magmatism in the collision sector of the Sunda–Banda arc, Indonesia. Geology 32, 41–44. https://doi.org/10.1130/G19941.1

Fadlin, Shaban, G., and Wildan, N.H., 2018. Active Continental Margin (ACM) Origin of tholeiitic magmatism in northern and southern Serayu-Banyumas, Central Java. Jurnal Geology dan Sumberdaya Mineral (JGSM), 19(1), 15-30.

Fadlin, Shaban, G., Ariyanti, N., Hamzah, W. N., and Aditama, M. R., 2021. Tholeiitic basalt in Banyumas Basin (Kebasen, Central Java): The evidence of sedimentary recycling input and the contribution of oceanic slab on fore-arc active continental margin (ACM) magmatism. IJOG, 8(2), 233-253. DOI:10.17014/ijog.8.2.233-253

Fadlin, Takahashi, R., Agangi, A., Sato, H., Idrus, A., Sutopo, B. et al., 2023. Geology, mineralization and calcite-rich potassic alteration at the Humpa Leu East (HLE) porphyry Cu-Au prospect, Hu'u district, Sumbawa Island, Indonesia. Resource Geology, 73(1), e12309. Available from: https://doi.org/10.1111/rge.12309

Foden, J.D. and Varne, R., (1980) The petrology and tectonic setting of Quaternary-Recent volcanic centres of Lombok and Sumbawa, Sunda arc: Chemical Geology, 30, 201–226.

Gardner, M.F., Troll, V.R., Gamble, J.A., Gertisser, R., Hart, G.L., And Rob M. Ellam, R.M., Harris, C., And Wolff, J.A., 2013. Crustal Differentiation Processes at Krakatau Volcano, Indonesia. Journal of Petrology, 54(1), 149-182. https://doi.org/10.1093/petrology/egs066

Garwin, S. L., 2002. The Geologic Setting of Intrusion-Related Hydrothermal Systems near the Batu Hijau Porphyry Copper-Gold Deposit, Sumbawa, Indonesia: Global Exploration 2002, Integrated Methods for Discovery, Colorado, USA. Society of Economic Geologists, Special Publication 9, 333-366. https://doi.org/10.5382/SP.09.15

Gertisser, R and Keller, J., 2003. Trace Element and Sr, Nd, Pb and O Isotope Variations in Medium-K and High-K Volcanic Rocks from Merapi Volcano, Central Java, Indonesia: Evidence for the Involvement of Subducted Sediments in Sunda Arc Magma Genesis. Journal of Petrology, 44(3), 457-489. https://doi.org/10.1093/petrology/44.3.457

Hamilton, W. B., 1979. Tectonics of the Indonesian Region. US Geology Survey Professional Paper 1078, Virginia, US.

Hattori, K., 2018. Porphyry copper potential in Japan based on magmatic oxidation state. *Resource Geology., 68*, p.126–137. https://doi.org/10.1111/rge.12160

Idrus, A., Kolb, J., Meyer, F.M., Arif, J., Setyandhaka, D., Kepli, S. (2009a) A Preliminary Study on Skarn-Related Calc-Silicate Rocks Associated with the Batu Hijau Porphyry Copper-Gold Deposit, Sumbawa Island, Indonesia. Resource Geology, 59 (3), 295-306.

Idrus, A., Kolb J. and Meyer F.M. (2009b) Mineralogy, Lithogeochemistry and Elemental Mass Balance of the Hydrothermal Alteration Associated with the Gold-rich Batu Hijau Porphyry Copper Deposit, Sumbawa Island, Indonesia. *Resource Geology,* 59

(3), 215–230.
Idrus, A., and Kolb, J. and Meyer, F.M. (2007). Chemical composition of rock-forming minerals in copper-gold-bearing tonalite porphyry intrusions at the Batu Hijau deposit, Sumbawa Island, Indonesia: Implications for crystallisation conditions and fluorine-chlorine fugacity. *Resource Geology*. 57, 102-113. https://doi.org/10.1111/j.1751-3928.2007.00010.x
Idrus, A,., Aji Syailendra Ubaidillah, I Wayan Warmada, and Syafruddin Maula., 2021. Geology, Rock Geochemistry and Ore Fluid Characteristics of the Brambang Copper-Gold Porphyry Prospect, Lombok Island, Indonesia. Journal of Geoscience (JGEET), 6(1). https://doi.org/10.25299/jgeet.2021.6.1.6145
Katili, J. A., 1975. Volcanism and plate tectonics in the Indonesian island arcs. Tectonophysics. 26, 3-4, 165-188. https://doi.org/10.1016/0040-1951(75)90088-8
Levashova, E.V.; Skublov, S.G.; Popov, V.A., 2021. Distribution of Trace Elements Controlled by Sector and Growth Zonings in Zircon from Feldspathic Pegmatites (Ilmen Mountains, the Southern Urals). *Geosciences*, *11*, 7. https://doi.org/10.3390/geosciences11010007
Li Huan, Xiao-Jun Hu, Safiyanu Muhammad Elatikpo, Jing-Hua Wu, Wei-Cheng Jiang, Wen-Bo Sun, Nuerkanati Madayipu., 2023. Zircon as a pathfinder for ore exploration. Journal of Geochemical Exploration, Volume 249. doi.org/10.1016/j.gexplo.2023.107216.
Maryono, Adi., Harrison, R. L., Cooke, D. R., Rompo, I., Hoschke, T. G., 2018. Tectonics and Geology of Porphyry Cu-Au Deposits along the Eastern Sunda Magmatic Arc, Indonesia. Economic Geology, 113, 7-38. https://doi.org/10.5382/econgeo.2018.4542
Martins, H.C.B. Sant'Ovaia, H. and Noronha, 2009. Genesis and emplacement of felsic Variscan plutons within a deep crustal lineation, the Penacova-Régua-Verín fault: an integrated geophysics and geochemical study (NW Iberian Peninsula). Lithos, 111, pp. 142-155
Martins, H.C.B. Sant'Ovaia, H. and Noronha, 2013. Late-Variscan emplacement and genesis of the Vieira do Minho composite pluton, Central Iberian Zone: Constraints from U–Pb zircon geochronology, AMS data and Sr–Nd–O isotope geochemistry. Lithos, 162/163, pp. 221-235
Martins, H.C.B., Simoes, P.P., and Abreu, J., 2014. Zircon crystal morphology and internal structures as a tool for constraining magma sources: Examples from northern Portugal Variscan biotite-rich granite plutons. *C. R. Geoscience, 346*, p.233-243. https://doi.org/10.1016/j.crte.2014.07.004
Myaing, Y., Idrus. A., Titisari A., 2018. Fluid Inclusion Studyof The Tumpangpitu High Sulfidation Epithermal Gold DepositInBanyuwangi District, East Java, Indonesia. Journal of Geoscience, Engineering, Environment, and Technology (JGEET), 3(1). https://doi.org/10.24273/jgeet.2018.3.01.1039
Nevolko, P.A., Svetlitskaya, T.V., Savichev, A.A., Vesnin, V.S., and Fominykh, P.A., 2021. Uranium-Pb zircon ages, whole-rock and zircon mineral geochemistry as indicators for magmatic fertility and porphyry Cu-Mo-Au mineralization at the Bystrinsky and Shakhtama deposits, Eastern Transbaikalia, Russia. *Ore Geology Reviews, 139,* Part B. https://doi.org/10.1016/j.oregeorev.2021.104532
PT STM., 2018. Internal Exploration Report and Discussion *(unpublished)*
Pupin, J. P., and Turco, G., 1972. Une typologie originale du zircon accessoire Bull. Soc. Fr. Mineral. Cristallogr., 95 (1972), pp. 348-359
Pupin, J. P., and Turco, G., 1975. Typologie du zircon accessoire dans les roches plutoniques, dioritiques, granitiques et syénitiques. Facteurs essentiels déterminant les variations typologiques. Petrologie, I (2), pp. 139-156
Pupin, J. P., 1980. Zircon and granite petrology Contrib. Mineral. Petrol., 110, pp. 463-472
Pupin, J. P., 1985. Magmatic zoning of Hercynian Granitoïds in France based on zircon typology. Schweiz. Mineral. Petrogr. Mitt., 65, pp. 29-56
Pupin, J. P., 1988. Granites as indicators in paleo-geodynamics. Rend. Soc. Ital. Mineral. Petrol., 43 (2), pp. 237-262
Ratman, N., & Yasin, A., 1978. Peta geologi regional lembar komodo, Nusatenggara. Pusat Penelitian dan Pengembangan Geologi.
Reubi, O., Nicholls, A. I., and Kamenetsky, V. S., 2002. Early mixing and mingling in the evolution of basaltic magmas: evidence from phenocryst assemblages, Slamet Volcano, Java, Indonesia. Journal of Volcanology and Geothermal Research, 119(1-4), 255-274. https://doi.org/10.1016/S0377-0273(02)00357-8
Richards, J. P., 2011. High Sr/Y arc magmas and porphyry Cu ± Mo ± Au deposits: Just add water. Econ. Geol. 106 (7), p.1075–1081. https://doi.org/10.2113/econgeo.106.7.1075
Richards, J. P., 2015. The oxidation state, and sulfur and Cu contents of arc magmas: Implications for metallogeny. *Lithos*, *233*, 27–45. https://doi.org/10.1016/j.lithos.2014.12.011
Rubatto, D., 2017. Zircon: The Metamorphic Mineral. Reviews in Mineralogy and Geochemistry, 83(1), 261–295. doi:10.2138/rmg.2017.83.9
Sillitoe, R.H. (2010). Porphyry Copper Systems. *Economic Geology*, *105(1)*, 3-41. https://doi.org/10.2113/gsecongeo.105.1.3
Sundhoro, H., Bakrun, Sulaeman, B., T., Sumardi, E., Imnuel, M., Risdiato, D. and Liliek, R. (2005) Survei Panas Bumi Terpadu (Geologi, Geokimia dan Geofisika) Daerah Hu'u, Kabupaten Dompu, Provinsi Nusa Tenggara Barat. *Prosiding Kolokium Hasil Laporan Lapangan-DIM*, 38, 1–10.
Sun, W. D., Huang, R.F., Li, H., Hu, Y. B., Zhang, C. C., Sun, S. J., Zhang, L. P., Ding, X., Li, C. Y., and Zartman, R.E., 2015. Porphyry deposits and oxidized magmas. *Ore Geol. Rev., 65,* 97–131. https://doi.org/10.1016/j.oregeorev.2014.09.004
Setijadji, L.D., Kajino, S., Imai, A., and Watanabe, K., 2006. Cenozoic island arc magmatism in Java Island (Sunda arc, Indonesia): Clues on relationships between geodynamics of volcanic centers and ore mineralization. Resource Geology, 56, 267–291. https://doi.org/10.1111/j.1751-3928.2006.tb00284.x
Setijadji, L.D., and Maryono, A., 2012. Geology and arc magmatism of the eastern Sunda arc, Indonesia: Indonesian Society of Economic Geologists (MGEI)

Annual Convention, Malang, Indonesia, November 26–27, 2012, Proceedings, 1–22.
Sudradjat, A., Andi Mangga, S., dan Suwarna, N., 1998. Peta Geologi Lembar Sumbawa, Nusa Tenggara, Skala 1: 250.000. Pusat Penelitian dan Pengembangan Geologi, Bandung.
Suratno, M., 1994. Peta Geologi dan Potensi Sumberdaya & Mineral Provinsi Nusa Tenggara Barat, Skala 1: 250.000, Kantor Wilayah Departemen Pertambangan dan Energi Nusa Tenggara Barat.
Turner BL, Kasperson RE, Matson PA, McCarthy JJ, Corell RW, Christensen L, Eckley N, Kasperson JX, Luers A, Martello ML, Polsky C, Pulsipher A, Schiller A., 2003. A framework for vulnerability analysis in sustainability science. Proc Natl Acad Sci U S A. 100(14):8074-9. doi:10.1073/pnas.1231335100.
Watson E.B., 1996. Dissolution, growth and survival of zircons during crustal fusion: Kinetic principles, geological models and implications for isotopic inheritance. Trans Roy Soc Edinburgh: Earth Sci 87:43-56. Also: Geol Soc Am Spec Paper 315:43-56